He 11 LIQUID/VAPOR PHASE SIWARA1OR FOR LARGE DYNAMIC RANGE OPERATION

A. Nakano*, D. Petrac, and C. l'sine

California Institute of '1'ethnology
Jet Propulsion Laboratory
4800 Oak Grove Drive
Pasadena, CA 91109-8099

ABSTRACT

A phase separator, which separates helium vapor from liquid superfluid helium (He II), is an indispensable device for space cryogenics. The most recent approach to the Space Infrared Telescope Facility (S1 RTF) uses a new design concept in which only the detector package is cold at launch, the remainder of the telescope being subsequently cooled to operating temperature on orbit, Therefore, a large dynamic operational range is required of the cryogen system. This is a report of initial laboratory test results with candidate porous plugs as phase separators. Mass flow rates and pressure and temperature differences across a porous plug were measured in this experiment. Relatively large mass flow rates were observed even at small pressure differences. In the high mass flow rate region, a hysteresis was observed with increases and decreases of the pressure difference. A linear theory is proposed and compared with experimental data to explain several phenomena observed in this system.

INTRODUCTION

A phase separator is of crucial importance for the efficient containment of He 11 for space missions[1,2]. A phase separator is composed of some sort of porous plug. The key mechanism to separate the vapor phase from the liquid He II is the thermomechanical effect, acting on the superfluid component, due to the temperature difference across a porous plug[3,4]. The superfluid component is driven toward tbc storage volume, where the temperature is higher than that at the space side where He II is evaporating. Consequently, the net mass flow rate of He II may be enough reduced to prevent bulk liquid He 11 from leaking out through a porous plug, because the superfluid component flows in the opposite direction to the net flow. It is important for the design of a cryostat to consider the basic characteristics of the mechanism for mass and heat transportation through the porous plug.

EXPERIMENTAL SETUP ANI) TEST PROCEDURES

A schematic illustration of the experimental setup is shown in Figure 1, The apparatus is composed of four parts: the porous plug, the helium dewar, the evacuation system for the main helium bath, and the porous plug's evacuation system. The helium dewar is made of glass to permit visual observation of the liquid/vapor phase boundary in the outer bath. The porous plug is fixed at the bottom of the evacuation tube, which is adjustable in the vertical direction to follow variations in the liquid level of the outer bath. A test porous plug is made of sintered stainless steel (Permaflow, Inc.). The diameter, d, is 25.4 x 10^{-3}m and the thickness, 1, is 6.3 x 10^{-3}m. The porosity E, the permeability κ_p, and the mean pore radius $\bar{R}$, are 0.21, 3.92 x 10^{-14}m^2, and 4. I x 10%, respectively. The $\bar{R}$ is calculated from a Blake-Kozcny equations. The porous plug is attached to its mount with a leak-tight iridium seal. The iridium closes some pores on the surface of the plug. The effective cross-sectional area, A, is 3.84 x 10^{-4}m^2 and this value is used for theoretical calculations,

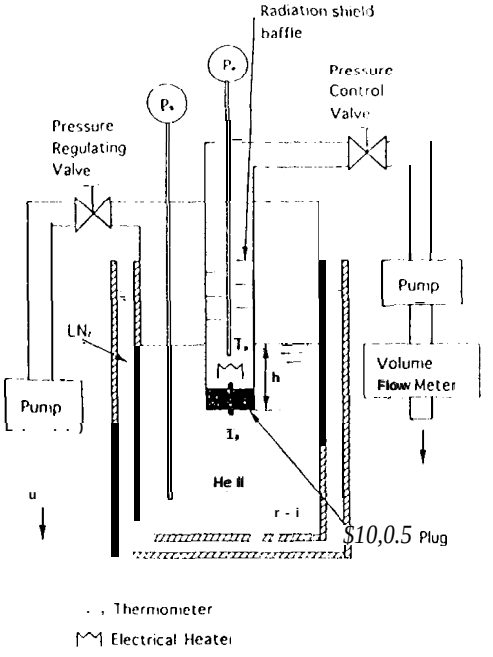

Figure 1. Schematic illustration of the experimental setup

The temperature of the helium bath and of the downstream side of the porous plug are measured by germanium resistance thermometers (GRTs). Each thermometer is excited by a 10 μA DC current. The pressure difference between these locations is measured by a precision piezo resistive pressure transducer. The volumetric flow rate is measured by a HASTING Model HFM 200H flow meter at the exhaust side of the evacuating pump. The mass flow rate, $\dot{m}$, is obtained by multiplying the measured volumetric flow rate by the density of helium gas under atmospheric conditions.

THEORETICAL CONSIDERATION OF THE PHASE SEPARATOR

When a phase separator is successfully operated and relatively high pressure or temperature difference is created across a plug, the liquid/vapor boundary may be located within the porous plug[6]. Therefore, we have to consider the heat and mass transport mechanism present in the vapor and liquid phases. In the case where the. entire plug is occupied with helium vapor, a mass flow rate is obtained from Darcy's law

$$\dot{m} = \frac{\rho_v A \kappa_p}{\eta_v l} \Delta P \tag{1}$$

1 lere, the p and η represent density and viscosity. The subscript v represents helium vapor. The AP stands for the pressure difference bet ween the upstream and the downstream sides of the porous plug. The equation suggests that the mass flow rate is proportional to AI' and the cross-sectional area of the porous plug, A, and is inversely proportional to length 1.

In the liquid phase, the heat and mass transport is described by the two fluid theory of the superfluid stale proposed by Landau. If the entire plug is occupied by liquid He 11, the mass flow rate, $\dot{m}$, is written as

$$\dot{m} = \frac{\rho_n^2 S T}{(L + ST)} \frac{A \kappa_p}{\eta_n l} \Delta P \tag{2}$$

1 lere, T, S, and L indicate temperature, entropy, and latent heat of vaporization, respectively. The subscript n indicates the normal fluid component.

We propose a model for the pressure distribution inside a porous plug, as shown in Figure 2.

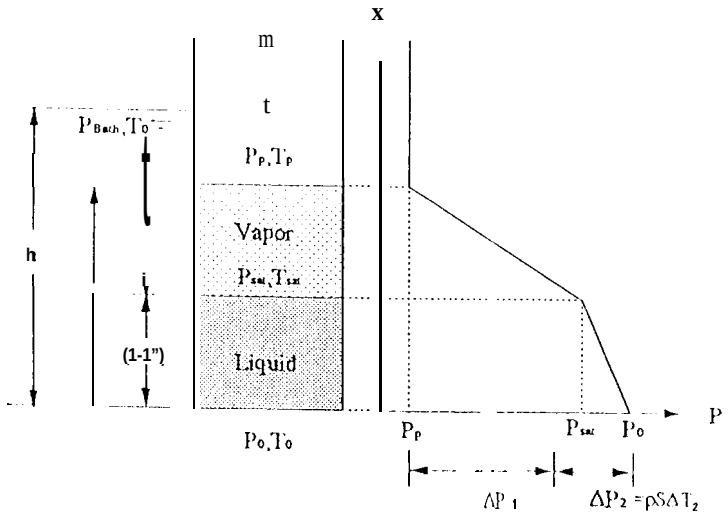

Figure 2. A model of pressure distibution in a porous plug

The location of the liquid/vapor phase boundary can be calculated from Eq. (1) as

$$l_v = \left\{\rho_v A \kappa_p / (\eta_V \dot{m})\right\}\left(P_{sat} - P_p\right) \tag{3}$$

The term IV represents the distance from the downstream surface of the porous plug to the liquid/vapor phase boundary. The term P_p is the pressure of the downstream surface of the porous plug, and P_{sat} is the vapor pressure of helium at the liquid/vapor boundary inside of the porous plug, which we write as

$$\begin{aligned} P_{sat} &= P_{bath} + \rho g h + \frac{2\sigma}{\bar{R}}\cos(\theta) - \rho S \Delta T_2 \\ &= P_O + \frac{2\sigma}{\bar{R}}\cos(\theta) - \rho S \Delta T_2 \quad \left(as\ P_O = P_{bath} + \rho g h\right) \end{aligned} \tag{4}$$

Here, σ is the surface tension of He II and θ is the contact angle between liquid and wall. The term g represents the acceleration due to gravity and h is the height of the liquid surface in the outer bath above the bottom of the porous plug. The term ΔT_2 is the temperature difference between the outer bath and the liquid/vapor phase boundary in the porous plug. The term $\rho g h$ is the hydrostatic pressure duc to the penetration depth of the porous plug. The term $2\sigma\cos(\theta)/\bar{R}$ accounts for the difference in saturated vapor pressure of a curved surface relative to that of a planer surface; within the pores, of radius $\bar{R}$, the fluid meniscus is assumed to have a spherical surface of radius $\bar{R}/\cos(\theta)$. The term $\rho S \Delta T_2$ stands for the thermomechanical pressure.

Wc note from Eq. (1) and Eq. (2) that these equations describe mass flow rate, flow resistance, and pressure gradient. This system is analogous to an electrical circuit. The mass flow rate, flow resistance, and pressure difference correspond to electrical current flow, electrical resistance, and voltage, respectively. The total resistance can be wr itten as

$$R = R_1 + R_2 = \frac{\eta_v l_v}{\rho_v A \kappa_p} + \frac{(L+ST)\eta_n}{\rho S T A \kappa_p}\left(l - l_v\right) \tag{5}$$

and the total voltage written as

$$V = V_1 + V_2 = \Delta P_1 + \Delta P_2 \tag{6}$$

where $AP_1 = (P_{sat} - P_p)$ and $\Delta P_2 = \rho S \Delta T_2$. The current, 1, is given by V/R, then a mass flow rate can be written as

$$\dot{m} = \left[\Delta P_1 + \Delta P_2\right] / \left[\frac{\eta_v l_v}{\rho_v A \kappa_p} + \frac{(L+ST)\eta_{nn}}{\rho S T A \kappa_{np}}\left(l - l_v\right)\right] \tag{7}$$

Substituting Eq. (3) into Eq. (7), it is found that

$$\dot{m} = \frac{A\kappa_p}{l}\left[\frac{\rho_v}{\eta_v}\Delta P_1 + \frac{\rho ST}{(L+ST)\eta_n}\Delta P_2\right] \qquad (8)$$

This is a very convenient model for the phase separation system because it allows us to consider the liquid and the vapor phases separately. But Eq. (8) is insufficient to describe a total mass flow rate of the real system, because the real system always has some heat leak from the downstream side of the porous plug, and the effect may be different for different systems. Thus, we propose following equation

$$\dot{m} = \frac{A\kappa_p}{l}\frac{\rho_v}{\eta_v}(P_o - P_p) + \frac{\rho ST}{(L+ST)\eta_n}(\rho S\Delta T_2) + \dot{m}_0(T) \qquad (9)$$

The $\dot{m}_0(T)$ corresponds to a creeping mass flow rate caused by a heat leak, which would, in general, be a function of temperature.

EXPERIMENTAL RESULTS AND DISCUSSION

General Flow Characteristics

The experimental data of mass flow rate, as plotted against the pressure difference, AP, between the upstream and the downstream side of the porous plug for several bath temperatures is shown in Figure 3a, It is found that the mass flow rate becomes small as the bath temperature decreases. It is also noted that a limit to mass flow rate seems to exist in the high pressure difference region', In the initial stage, the mass flow rate increases even though the pressure difference is very small. We call this region the 'initial region'. A hysteresis in the relationship is seen with increases and decreases in the pressure difference, The upper branch seems nonlinear and the lower branch seems linear. Hereafter, we will call the upper branch the 'nonlinear region' and the lower branch the 'linear region'. Figure 3b show-s- the relationship between the mass flow rate and temperature difference, ΔT. The initial region and the hysteresis are also observed in this figure.

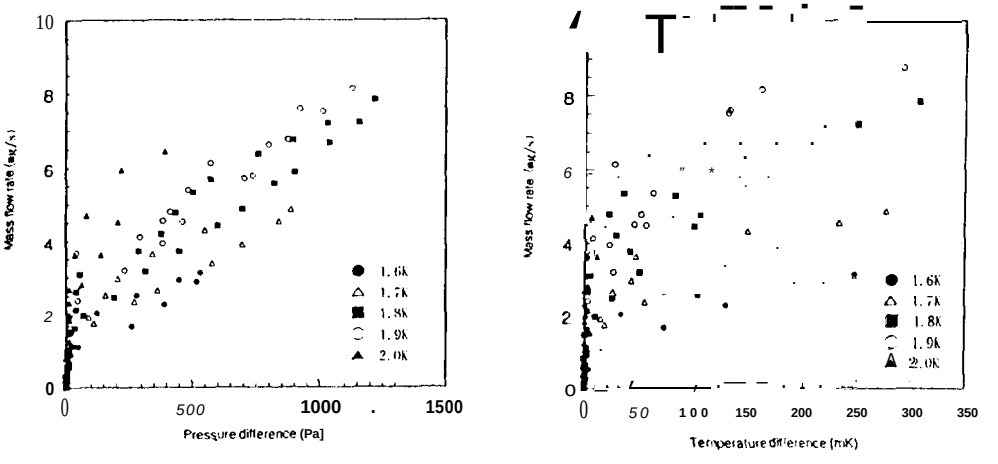

Figure 3. General steady-flow characteristics through a porous plug
a) mass flow rate $\dot{m}$ - pressure difference AP
b) mass flow rate $\dot{m}$ - temperature difference Al'

The Initial Region

1'0 investigate the initial region more minutely, mass flow rates at the triple points, where the initial, nonlinear, and linear region lines intersect, are plotted against T_B in Figure 4.

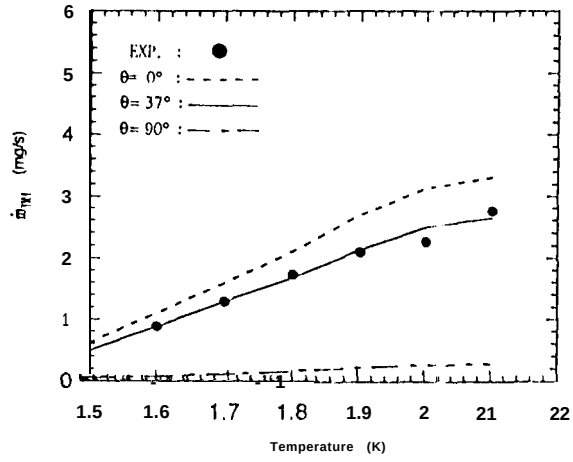

Figure 4. The variation of mass flow rate at the triple point in the initial region with bath temperature T_B.

It is seen that the measured flow rate tends to increase with increases in the bath temperature. The theoretical prediction is compared with the experimental data. The $\dot{m}_{IRI}$ is calculated from the following: in the initial region, the liquid/vapor phase boundary is assumed to be located at the upper surface of the porous plug, i.e., the plug is completely filled with liquid. That way, the P_{sat} and ΔT_2 in Eq. (4) correspond to P_p and ΔT, respectively, here

$$\rho S \Delta T = P_{bath} - P_l + \frac{2\sigma}{R}\cos(\theta) + \rho g h = \left\{\frac{dP}{dT}\right\}_{svp} \Delta T + \frac{2\sigma}{R}\cos(\theta) + \rho g h \qquad (10)$$

Rewriting Eq. (10), we find

$$\Delta T = \left[\frac{2\sigma}{R}\cos(\theta) + \rho g h\right] \Big/ \left[\rho S - \left\{\frac{dP}{dT}\right\}_{svp}\right] \qquad (11)$$

From Eq. (2), Eq. (11), and the London equation, $\Delta P = \rho S \Delta T$, the $\dot{m}_{IRI}$ is obtained as follows

$$\dot{m}_{IRI} = \frac{(\rho S)^2 A \kappa_p}{(L + \Delta T)\eta_n} \cdot \frac{\frac{2\sigma}{R}\cos(\theta) + \rho g h}{\rho S - \left\{\frac{dP}{dT}\right\}_{svp}} \qquad (12)$$

The broken line and the dash/dot line in Figure 4 show the theoretical prediction in the case of $\theta = 0$ and $\theta = 90°$, respectively. The best-fitting, contact angle of the triple point is $\theta = 37°$, which is shown by the solid line, At each point on the line in the initial region, the capillary force is different because of the different contact angle*. The contact angle at the triple point seems to be the same as the contact angle in the linear region. It is found from this figure that a liquid/vapor phase boundary is always located at the upper surface of the porous plug in the initial region.

Hysteresis

The experimental data show a hysteresis in the high mass flow region. To investigate this hysteresis, we have repeatedly cycled the pressure difference through the range shown in Figures 5a and 5b. Figure 5a shows the relationship between the mass flow rate, $\dot{m}$, and pressure difference, AP, and Figure 5b shows the relationship between $\dot{m}$ and temperature difference, AT. The experimental data suggest that the upper branch has some broadening, suggesting that the upper branch is unstable. The lower branch is relatively stable compared with the upper branch. In the case of equal total pressure difference or temperature difference, the mass flow rate in the nonlinear region is larger than that in the linear region. We explain the existence of hysteresis as follows: As the pressure on the downstream side decreases sufficiently, the porous plug behavior moves from that of the initial region to that of the upper branch, which we are calling the nonlinear region. Increased evaporation produces an increase in ΔT_2, which drives the liquid/vapor interface into the bulk of the

porous plug. We expect the meniscus contact angle to be very small in this case, as the liquid/vapor interface retracts from the previously wetted surface. Conversely, if the downstream pressure increases, the evaporation rate and the temperature difference decrease, thus the liquid/vapor interface moves back toward the downstream face of the porous plug.

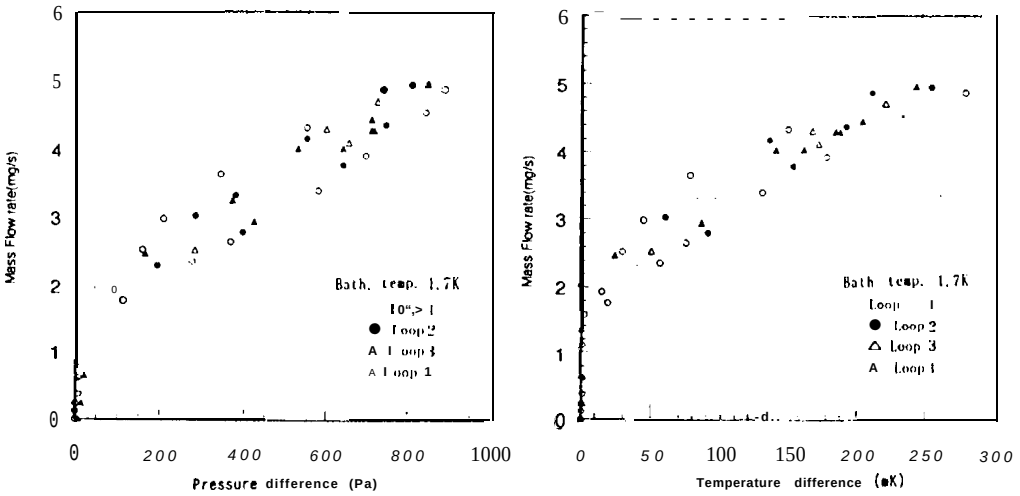

Figure 5. Examination of hysteresis behavior
a) mass flow rate $\dot{m}$ - pressure difference ΔP
b) mass flow rate $\dot{m}$ - temperature difference ΔT

In this case the liquid is moving onto a previously dry surface, and we expect the contact angle to be larger. It is this variation in contact angle with change in direction of the liquid/vapor interface motion which gives rise to the two branches of the mass flow rate curve, through the change in vapor pressure with surface curvature. The greater stability of the linear branch suggests that the interface is more stable when advancing onto a dry surface.

The Linear Region and the Nonlinear Region

A phase separator is mainly operated in a high mass flow rate region. Therefore, it is important to investigate the flow characteristics in these regions. From Eq. (9), we can consider the effect of the liquid phase and the vapor phase each separately. Figure 6 shows the relationship between ΔP and ΔT for several bath temperatures. There is no hysteresis indicated in this figure. The solid curves indicate saturation vapor pressure. All experimental data fall just below these lines. This suggests that the phase in the downstream side of the porous plug is vapor.

The slope of the curve from experimental data in the linear region is compared with the theoretical prediction in Figure 7. The solid line shows the theoretical prediction of the vapor phase and the broken line shows that of the liquid phase. The quantities ρ_v and η_v should be chosen from $T = (T_{sat} + T_p)/2$. But we use data for T_{sat} here for simplicity because each experimental data set has a different T_p. The experimental data points are always located between these two lines, The experimental data do not agree with the broken line and fall near the solid line except in the high temperature region. This disagreement in the high temperature region is caused by a limitation in our experimental setup. This figure suggests that the effect of the vapor phase is much more dominant than that of the liquid phase in the linear region. It can be also predicted from this figure that the magnitude of hysteresis becomes small as the bath temperature decreases, because the broken line approaches the solid line. In fact, the feature can be observed in Figures 3a and 3b.

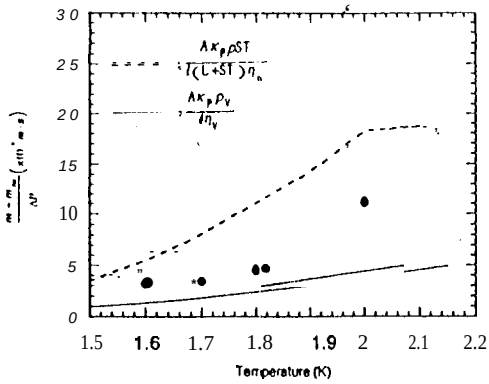

Figure 6. Comparison of experimental data with saturation vapor pressure T_{B+}

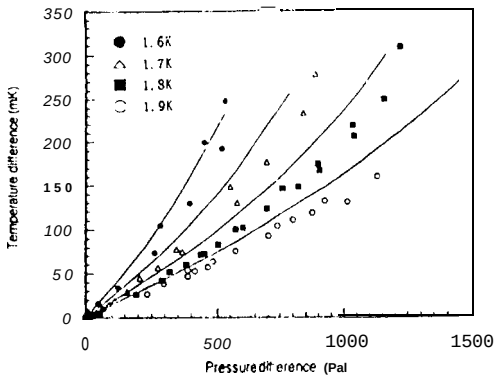

Figure 7. Variation of flow conductance with bath temperature T_{B+}

The Effect of Gravity

Figure 8a shows the relationship between $\dot{m}$ and AP for the different hydrostatic pressure heads h = 1 cm and 10 cm, respectively.

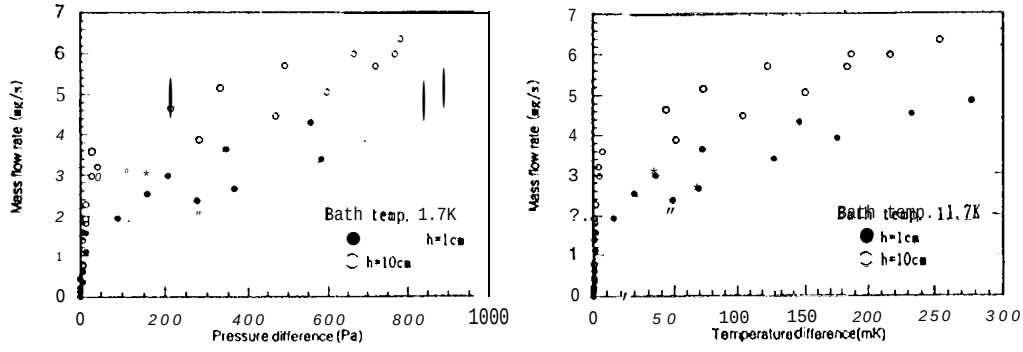

Figure 8. The effect of pressure head due to gravity
a) mass flow rate $\dot{m}$ - pressure difference ΔP
b) mass flow rate $\dot{m}$ - temperature difference Al'

Figure *8b* shows the relationship between $\dot{m}$ and temperature difference AT. in the case of a high hydrostatic pressure head, the mass flow rate $\dot{m}$ is larger, clearly suggesting the effect of gravity on the mass flow rate. The theoretical model also predicts this effect, By using Eq. *(4), (9),* and (10), the total mass flow rate $\dot{m}$ can be written as

$$\dot{m} = \frac{A\kappa_p}{l}\left[\frac{\rho_v}{\eta_v}\left(P_{bath} - P_p - \left\{\frac{dP}{dT}\right\}_{svp}\Delta T_2\right) + \frac{\rho ST}{(L+ST)\eta_n}\left(\left\{\frac{dP}{dT}\right\}_{svp}\Delta T_2 + \rho gh + \frac{2\sigma}{R}\cos(\theta)\right)\right] + \dot{m}_0(T) \quad (13)$$

Here, P_{bath}, P_p, and $\frac{2\sigma}{R}\cos(\theta)$ arc constant. If the hydrostatic pressure causes an increase in Ah, the increment of mass flow rate, $\Delta\dot{m}$, can be calculated from the equation shown above and from Eq. (11) as

$$\Delta\dot{m} = \frac{A\kappa_p}{l}\left[\frac{(/3s)^2 7'}{(L+ST)\eta_n\left(\rho S - \left\{\frac{dP}{dT}\right\}_{svp}\right)} - \frac{\rho_v\left\{\frac{dP}{dT}\right\}_{svp}}{\eta_v\left(\rho S - \left\{\frac{dP}{dT}\right\}_{svp}\right)}\right]\rho g\Delta h \quad (14)$$

Theoretical prediction suggests that the 9 cm hydrostatic pressure difference produces 1.1 $mg \cdot s^{-1}$ increased mass flow rate. The experimental data show fairly good agreement with this value. Eq. (14) predicts that $\Delta\dot{m}$ should have a temperature dependence. This has not been observed yet. Further investigation and more experimental data are required to investigate this effect.

SUMMARY AND FUTURE WORK

The basic characteristics of a porous plug have been investigated and the following conclusions were made:

1. Three different flow regions are observed from this experiment and a limit of mass flow rate seems to exist for large pressure differences.
2. In the initial region, it can be considered that a liquid/vapor phase boundary is always located at the downstream surface of the porous plug.
3. The nonlinear region and the linear region exhibit hysteresis. The linear region is relatively stable compared with nonlinear region. The hysteresis is produced by variations in the capillary force caused by changing contact angles.
4. The effect of the vapor phase is more dominant than that of the liquid phase under relatively high pressure- and temperature-difference conditions in the linear region.
5. The magnitude of hysteresis becomes small as the bath temperature decreases.
6. The effect of hydrostatic pressure due to gravity is understood from simple linear theory. The theoretical predictions show good agreement with experimental data.

This experimental set-up has two evacuation systems. One serves porous-plug portion of the setup and the other maintains a constant bath temperature. But, in the case of an actual space mission, there is only one evacuation line for bath temperature control that is downstream of the porous-plug. We have a plan to test porous plugs by using just one evacuation line. This will allow us to obtain more useful data for the design of a space application cryostat.

ACKNOWLEDGEMENT

The work described in this paper was performed at the Jet Propulsion Laboratory, California Institute of Technology, under a contract with the National Aeronautics and Space Administration. This work was partially supported by the Japan Society for the Promotion of Science. The authors thank Dr. D. Elliott and Mr. S Kikkert for their information about the Janis test dewar. We wish to give special thanks to Prof. M. Murakami of the University of Tsukuba for useful suggestions. Also, we extend thanks to JPL, Mr. S. Elliott for technical assistance.

* Supported by the Japan Society for the Promotion of Science. Visiting JPL scientist from University of Tsukuba, Japan.

REFERENCES

1. D. Petrac and P. Mason, "Infrared Astronomical Satellite (IRAS) Superfluid Helium Tank Temperature Control", Proceedings of the 1983 Space Helium Dewar Conference, University of Alabama (Huntsville), (1984), p. 163.
2. D. Petrac, "Low Temperature Platform Cryostat Performance", Proceedings of the NASA/JPL 1994 Microgravity Low Temperature Physics workshop, (1 994), p.353.
3. M. Murakami, N. Nakaniwa, H. Nakai, and K. U yama, "1 Experimental Study on Porous-Plug Phase Separator for Superfluid He 11", The ISAS Report, No. 612, 1 (1984).
4. J .B. Hendricks and G.R. Karr, "Superfluid Porous Plug Performance", Proceedings of the 1983 Space Helium Dewar Conference, University of Alabama (Huntsville), (1984), p.133.
5. R.B. Bird, W.E. Stewart, and E.N. Lightfoot, "Transport Phenomena", John Wiley and Sons, New York, (1960).
6. H. Nakai and M. Murakami, "Flow Phenomena of Superfluid 1 Helium Through a Porous Plug Phase Separator", Cryogenics 27, 442 (1987).
7. J.B. Hendricks and G.R. Karr, "The Liquid/Vapor Transition in Porous Plug Operation", Adv. Cryo. Eng. 31,861 (1986).
8. M .J. Dipirro and J. Zahniser, "The Liquid/Vapor Phase Boundary in a Porous Plug", Adv. Cryo. Eng. 35, 173 (1990).